Intelligent MRI Analysis for Parkinson's Disease Detection

R. Indhumathi¹, Alaa A. ELnazer^{2,†}, Sharvari R. Shukla³, Showkat A. Dar⁴, Hela Hakim⁵, A. Vijaya Mahendra Varman⁶, Tanvir Habib Sardar⁷ and Aafaq A. Rather^{3,*}

Abstract: This study presents a practical approach for classifying Magnetic Resonance Imaging (MRI) scans to distinguish between normal subjects and those affected by Parkinson's disease (PD). PD is a progressive brain disorder marked by dopamine deficiency, and lacks reliable diagnostic methods for early detection. To overcome this challenge, we employed Scale-Invariant Feature Transform (SIFT) and Local Binary Pattern (LBP) in designing a Computer-Aided Diagnostic (CAD) System. The extracted features are classified using K-Nearest Neighbour (KNN) and Decision Tree algorithms. Experimental results show that LBP features classified through the Decision Tree achieved the highest accuracy of 97.41%, demonstrating the efficiency of the proposed method in achieving early and accurate detection of PD.

Keywords: MRI Classification, Computer Aided Diagnosis, SIFT, LBP, KNN.

1. INTRODUCTION

A neurological disorder that predominantly affects older adults is PD [1]. In addition to causing tremors, slowness, muscle imbalance, and stiffness, it also alters a person's speech [2]. The symptoms of PD can be divided into many categories. Symptoms that are both motor and non-motor. Humans can visually notice the motor signs. The symptoms include stiffness, postural instability (balance issues), bradykinesia (slow movement), and resting tremor. These symptoms and other biomarkers from Cerebrospinal Fluid Measurement (CSF) and dopamine transporter imaging help us predict PD. Non-motor symptoms include cognitive impairment, loss of sense of smell, sleep difficulties, constipation, unexplained pains, speech and swallowing problems, drooling, and blood pressure when standing. Figure 1 shows the sample image of a Parkinson-affected brain MRI image.

Even though methods like dopamine transporter single photon emission computed tomography (SPECT) and DaTSCAN imaging are known to help

diagnose Parkinson's disease, their use is still restricted in many clinical settings due to high cost, radiation exposure, and difficulty. Instead of being used for early-stage detection, these modalities are frequently used for confirmation.

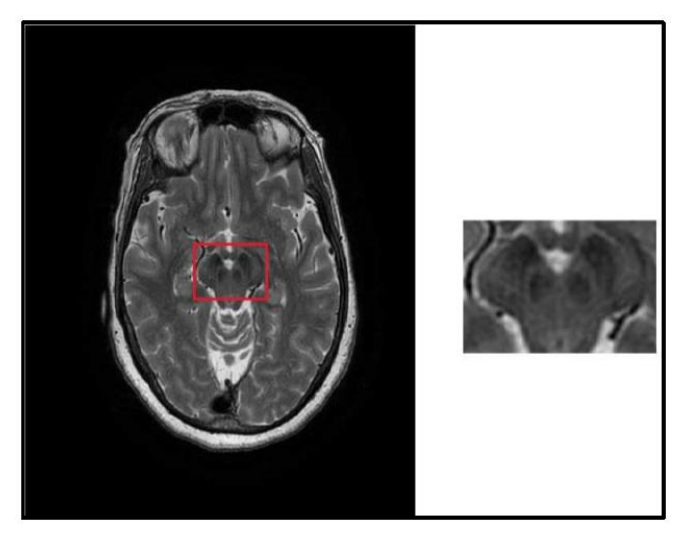


Figure 1: Sample MRI image of Parkinson's disease.

To fill this gap, the proposed MRI-based Computer-Aided Diagnosis (CAD) system utilizes SIFT and LBP feature extraction with Decision Tree and KNN classifiers to provide an automated, affordable, and

¹Department of Al/ML, Department of Computer Science, Idhaya College for Women, Kumbakonam, India

²Department of Marketing, College of Business, Imam Mohammad Ibn Saud Islamic University (IMSIU), Riyadh 11432, Saudi Arabia

³Symbiosis Statistical Institute, Symbiosis International (Deemed University), Pune, India

⁴Department of Computer Science and Engineering, GITAM University Bangalore Campus -561203, India

⁵Researcher Associated with the MIRACL Laboratory, University of Sfax, Tunisia-3029

⁶Department of Artificial Intelligence and Data Science, Panimalar Engineering College-600 123, Chennai, India

⁷Department of CSE, School of Engineering, Dayananda Sagar University, Bengaluru–562112, India

^{*}Address correspondence to this author at the Symbiosis Statistical Institute, Symbiosis International (Deemed University), Pune, India;

E-mail: aafaq7741@gmail.com

[†]E-mail: aaelnazer@imamu.edu.sa

Figure 2: Proposed Architecture of Parkinson's disease Classification.

repeatable approach for early PD detection. By using Intelligent image analysis to increase early recognition and classification accuracy, this method seeks to complement current diagnostic tools.

It is the second most frequent neurological condition that primarily affects older people. Although this disease's primary cause is unknown, environmental, and genetic factors play a role. In the proposed work, SIFT and LBP were employed for feature extraction. Then the derived features are given to KNN (K Nearest Neighbor), Decision Tree which classifies the Parkinson's images into regular/abnormal classes is discussed. Figure 2 displays the overall framework of normal/abnormal classification.

2. BACKGROUND LITERATURE

PD is predicted to increase in prevalence based on the current pattern of ageing social behaviour. Even though this disease has no known cure, early treatment with the right drug can significantly reduce symptoms. There is a strong desire to employ classification methods for PD detection because the conventional approach is too intrusive, extensive, and complex for self-use.

Kamal Nayan Reddy Challa describe a PD detection method that uses the connection weights of interconnections between neurons in ANNs to spread knowledge about the problem [3]. The neural network must be trained to modify the biases and connection weights to obtain the proper mapping. Modeling, data analysis, and diagnostic detection are common uses of ANNs in the biomedical field. The ANN model's training algorithm is very significant. A good training algorithm has a short learning curve and achieves higher accuracy.

Pir Masoom Shah developed the PD identification technique. Because of its unique qualities, such as self-learning, flexibility, robustness, and massive parallelism, many researchers have chosen the Artificial Neural Network as the classification method [4]. It is made up of several interconnected computational neural units.

According to Zehra Karapinar Senturk, Fuzzy logic can take vague or imprecise observations as inputs and produce crisp and precise results. A Fuzzy Inference System (FIS) was created using the subtractive clustering methodology [5].

Anitha S. used a greater number of clusters and cluster centres in the dataset images, determined through a clustering algorithm. The Fuzzy Inference System (FIS) includes inputs, outputs, and a collection of rules that define how the system behaves. Each input and output contain as many membership functions as there are clusters. The radius parameter specifies how far the influence of a cluster centre extends in each data dimension. After training, the FIS structure is formed with a set of fuzzy rules that span the feature space, which is then applied to perform fuzzy inference on the test data [6].

Recent studies have increasingly investigated machine learning and deep learning techniques applied to neuroimaging data for Parkinson's disease detection, in addition to traditional Artificial Neural Networks (ANNs) and models based on fuzzy logic. The potential of hierarchical feature learning for enhanced pattern recognition in MRI and functional imaging data has been shown in studies using Convolutional Neural Networks (CNNs) and autoencoder-based feature extraction [14–18]. In contrast to hand-crafted features, CNN models have

been used to automatically extract spatial features from 3D MRI volumes, improving diagnostic performance. Other research has combined classical classifiers with wavelet-based, Gabor filter, and histogram of oriented gradients (HOG) features, and has achieved high sensitivity in distinguishing PD from healthy subjects.

Despite these developments, the routine clinical application of many deep learning techniques is restricted by their computational costs and requirement for sizable annotated datasets. In this regard, this research presents a hybrid MRI-based CAD framework that uses SIFT and KNN classifiers, offering a computationally effective and comprehensive substitute for accurate PD diagnosis based on structural MRI data.

3. METHODOLOGIES

3.1. Feature Extraction Techniques

The process of feature extraction begins after the input photos have been read. Feature extraction is a method for indexing and retrieving captured images' visual content [7].

3.1.1. Scale Independent Feature Detection (SIFT)

The stable features are obtained through the SIFT technique. The features obtained through retrieval are affine modification, lighting, rotation, and scaling, which are resistant to sub-pixel precision [8]. The algorithm follows four steps, which are discussed below.

- Assigning orientation
- Localizing key points
- Defining extrema across different scales
- Describing the key points

Then, the 128-dimensional descriptors are matched against it. SIFT is a very efficient technique for feature extraction from photomicrographic images [9].

Identification of Extrema with Scale Space

It creates the Gaussian "scale space" for an input image. Gaussian functions of varying widths are applied to the image to create a convolution in Eqs. (1) and (2), it is defined as $L(x,y,\sigma)$ that yields the convolution of a variable-scale Gaussian, $G(x,y,\sigma)$, of an input image I(x,y).

$$L(x, y, \sigma) = G(x, y, \sigma) * l(x, y)$$
(1)

Here, x is the convolution function in x and y, and

$$G(x,y) = \frac{1}{2\pi\sigma^2} - e^{(x^2 + y^2)} / 2\sigma^2$$
 (2)

The distinction between D (x, y, σ) computes the difference of two neighbouring scales divided by a persistent multiplicative factor k, as provided in Eqs. (3) and (4).

$$DoG(x, y, \sigma) = (G(x, y, k\sigma) - G(x, y, \sigma) * l(x, y))$$
(3)

$$DoG(x, y, \sigma) = L(x, y, k\sigma) - L(x, y, \sigma)$$
(4)

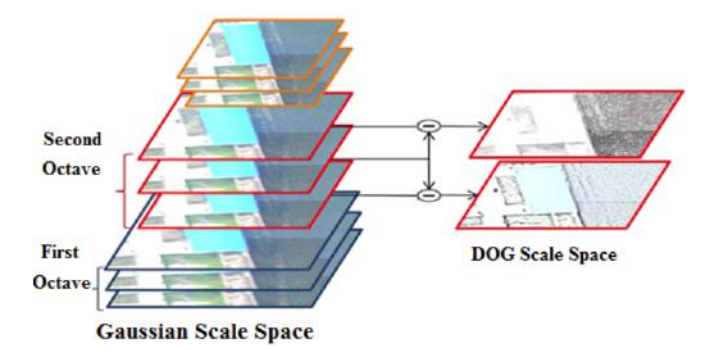


Figure 3: SIFT Scale Space.

This function is primarily helpful for processing smoothed images, where L must be computed in the case of scale space feature description. Then, as shown in Figure 3, DoG is calculated by image subtraction, and each point is compared with its eight neighbors up and down one scale to determine the maxima and minima of DoG (x, y, σ) , as shown in Figure 4.

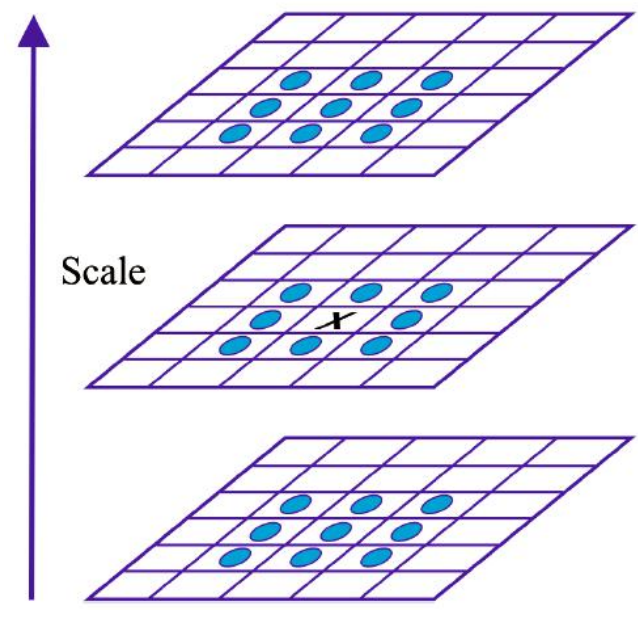


Figure 4: Scale Space Key Point Detection.

This value is referred to as an extrema when it represents the lowest or greatest of all these locations.

Key Point Localization

Identifying the key point from an image's low contrast or poorly localised edge is known as "key point localisation." Equation (5) represents the value of the DOG pyramid's essential points at the extrema.

$$D(Z) = D + \frac{1}{2} \frac{\partial D^{-1}}{\partial x} Z \tag{5}$$

This point is excluded when the value of Z falls below the threshold. To eliminate poorly localized extrema, a primary curve is applied along the edge. The difference of the Gaussian function is then given a small curvature in the perpendicular direction. At each location, a 2x2 Hessian matrix (as shown in Eq. 6) is calculated and the key points are used to determine the curvature, allowing it to be computed efficiently.

$$D = \begin{bmatrix} D_{xx} & D_{xy} \\ D_{xy} & D_{yy} \end{bmatrix}$$
 (6)

Orientation Assignment

The main features of the local picture attributes are used to determine the orientation. The gradient orientation of the sample points inside the area surrounding the key points is used to create a histogram. Thirty-six bins, spanning a 360-degree range of orientations, comprise the orientation histogram. Pixel versions in Eqs. (7) and (8) are used to process the gradient magnitude, m(x,y), and orientation, i(x,y).

$$m(x,y) = \sqrt{\frac{L(x+1,y) - L(x-1,y)^2 + 1}{(L(x,y+1) - L(x,y-1))}^2}$$
(7)

$$\theta(x,y) = a \tan 2(L(x,y+1) - L(x,y-1), L(x+1,y) - L(x-1,y))$$
(8)

A Gaussian-weighted circular window with a "o" that is 1.5 times the scale of the key points and the gradient magnitude is used to weigh each sample. The orientation histogram's peaks correspond to the local gradients' principal directions. Key points with that orientation are created using the highest peak in the histogram. To improve accuracy, the position of each peak is interpolated by matching the three histogram values closest to a Gaussian Distribution. This determines the SIFT features' scale, orientation, and

position in the image. The corners and intensity gradients have a profound effect on these traits.

Key Point Descriptor

The core concept involves computing the descriptor for the image region around each potential key point. The critical point position takes samples of the image's gradient and magnitude. σ is utilised to relate to the measure of the key points to establish a weight to the magnitude of a Gaussian weighting function. Rotating the descriptor and gradient orientation coordinates to the key point orientation yields the orientation invariance. The 16 × 16 image is seen in Figure 5. We consider 4 × 4 blocks in our studies, which produces a 4 × 4 × 8-dimensional feature vector.

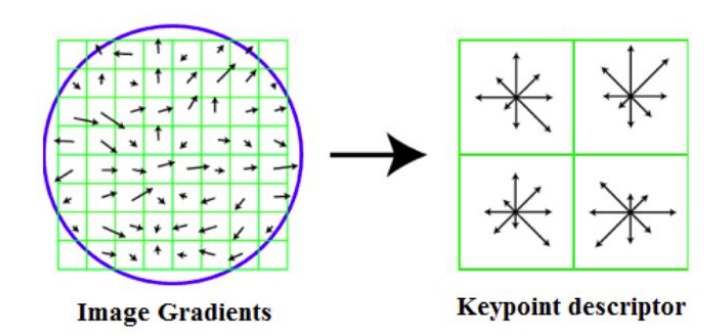


Figure 5: Building Key point.

By merging image gradients into orientation histograms from 4×4 subregions, a 128-dimensional SIFT feature vector is produced, in which each of the 8 directional bins represents the dominant edge strength and orientation in its surrounding area.

3.1.2. Local Binary Pattern (LBP)

The LBP is a popular technique for extracting texture features from images. It represents local textures by comparing each pixel with its neighborhood pixels [10]. This method involves the following steps:

Algorithm of LBP

- In order to convert the image into greyscale, we first create an LBP texture description.
- The LBP descriptor works in the fixed 3 x 3 pixel neighborhood.
- We consider the centre pixel and compare it with the eight surrounding pixels.
- We assign the value one if the intensity of the centre pixel is 8 bits or more than or equal to that of its neighbour.

- The LBP value of the centre pixel is computed either in a clockwise or anti-clockwise direction.
- The binary test is performed for a 3 x 3 neighborhood with 8 neighbors.
- After storing in an 8-bit array, the binary test result is translated into a decimal value.
- If LBP contains no more than 0-1 or 1-0 transitions, it is considered uniform.
- For each input image pixel, thresholding, accumulation of binary strings, and storage of the output decimal value in the LBP array are iteratively performed.
- Then the histogram of the output LBP array is computed.
- Because there can be 28 = 256 possible patterns in 3 x 3 neighborhoods, 0 is the lowest and 255 is the highest.
- So, we constructed a 256-bin LBP histogram.

Finally, the output array has the calculated value

Therefore, the LBP descriptor of each pixel is represented as follows:

$$LBP(P,R) = \sum_{p=0}^{p-1} f(g_p - g_c) 2^p$$
 (9)

Where g_p and g_c indicates the pixel intensities of the present and nearby pixels, P is the nearby pixel count chosen at the radius R.

Following previous work in medical texture analysis [10,11], a 3 × 3 neighbourhood configuration for the LBP operator was chosen because it effectively captures micro-textual variations without being oversensitive to noise. Large neighborhoods such as 5×5 or 7×7 in pilot testing result in a significant increase in computational cost but no discernible improvement in classification accuracy. Therefore, the 3 × 3 arrangement offered the best possible balance between feature compactness, resilience to change in illusion, and accurate depiction of the fine-grained textures typical of brain tissue affected by PD.

3.2. Modeling the Features

3.2.1. K-Nearest Neighbor Algorithm (KNN)

KNN algorithm is a type of supervised learning method applied in statistics, data mining, and many other fields. KNN classifies objects by analysing the nearest training samples in feature space and assigning the label based on the majority of its neighboring points [12]. The algorithm below computes K nearest neighbors.

- Find the number of nearest neighbors, represented by the parameter K.
- Use the Euclidean distance method to determine the distance between the query instance and each training sample.
- Sort all the training samples' distances, then use the K-th minimal distance to get the closest neighbor.
- Get all the categories of the training data for the sorted value that falls under K.
- Use the majority of nearest neighbors as the prediction value.

3.2.2. Decision Tree

A decision tree is a supervised learning model that uses tree like rules from training data to predict target outcomes.

By placing the samples from the tree's root down to a leaf or terminal node, which provides categorisation, the Decision Tree separates the samples.

Determining which features must be considered the root node at each level is the main issue in the Decision Tree implementation. Finding the attribute selection is how this is handled. Various attribute selection measures are used to identify the feature that can be thought of as the root node at each level. Figure 6 displays the Decision Tree architecture.

Decision Tree Algorithm

- 1. Divide the data according to the most significant feature using Attribute Selection Measures (ASM).
- Divide the dataset into smaller subgroups and make that feature a decision node.
- 3. Continue doing this repeatedly for every child until one of the prerequisites is met to begin constructing the tree.

There are no more instances or surviving attributes: all tuples pertain to the same attribute value.

Figure 6: Decision Tree Architecture.

Attribute Selection Measures

The attribute selection measure is a heuristic used to identify the optimal splitting rule for effective partitioning of data. ASM defines the provided dataset and assigns a rank to each attribute. The attribute with the highest score will be chosen as a splitting attribute. The most widely used selection criteria are

- Information Gain
- Gain Ratio
- Gini Index

In this proposed work, the Gini Index is used for attribute selection.

4. EXPERIMENTAL RESULTS

4.1. Datasets

The study utilizes datasets from Kaggle repository, comprising 751 images, -395 normal and 356 Parkinson's affected, for training, while 192 images were tested using KNN and Decision tree classifiers.

This study utilizes MRI data from The "Parkinson's Disease MRI Dataset" on Kaggle (https://www.kaggle.com/datasets/nidaguler/parkinson's-disease-mri-dataset) is the source of the MRI data used in this study. Of the 943 T1-weighted brain MRI images in the dataset, 751 (395 normal and 356 Parkinson 's-affected) were used for training, while 192 were set aside for testing. The axial plane is used for all MRI scans, with a primary focus on the substantia

nigra and basal ganglia, two clinically significant regions known to show structural abnormalities in Parkinson's disease.

Prior to feature extraction, each image was resized to 256×256 pixels and grayscaled. In order to standardize image quality and lower noise throughout the dataset, pre-processing techniques included intensity normalization, background removal, and contrast enhancement using histogram equalization. No personally identifiable information about the patient was kept.

4.2. Environmental Setup

Previous studies have also highlighted the importance of optimized deep learning environments for medical imaging applications [13].

Installing Python 3.6 and the Anaconda library created a deep learning environment. The OpenCV-Contrib (v3.3.0) library was successfully integrated with the Python interpreter. The Conda install command was used to install Keras and the TensorFlow backend, and pip was used to import necessary libraries, including NumPy, PIL, Scikit-Learn, SciPy, sklearn, and pickle.

4.3. Performance Measures

Accuracy, precision, recall, and F-score are among the evaluation metrics used in this study; they are all obtained from the confusion matrix produced during the classification procedure.

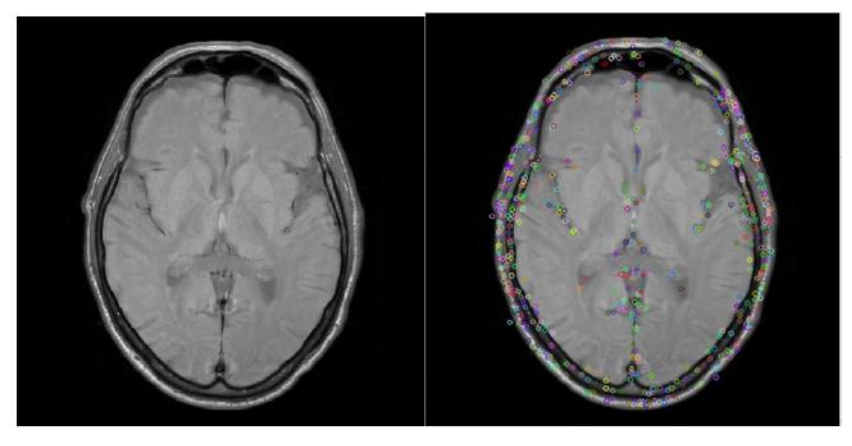


Figure 7: Original image and SIFT key points image.

Accuracy

A measurement system is considered accurate if it produces truthful data (no systematic mistakes) and consistent (no random errors).

$$Accuracy = \frac{TP + TN}{TP + TN + FP + FN} \tag{10}$$

Precision

In Classification tasks, precision measures how accurately positive predictions are made. It is calculated as the ratio of true positives to the total predicted positive(true positive plus false positive)

$$Precision = \frac{TP}{TP + FP} \tag{11}$$

Recall

Recall is defined as the ratio of true positives to actual positives in the dataset.

$$Recall = \frac{TP}{TP + FN} \tag{12}$$

F-Measure

F-measure is an accuracy metric that represents the harmonic mean of

$$F - Measure = 2 \frac{Precision * Recall}{Precision + Recall}$$
 (13)

4.3.1. Performance of SIFT with KNN and Decision Tree

In the proposed work, SIFT points are detected, extracted, and given to the KNN and Decision Tree classifiers. The image input has been scaled to 256 \times 256 with a window size of 4 \times 4. SIFT generates a 128-dimensional feature vector by taking eight orientations.

KNN and Decision Trees are given the 128dimensional feature vector. Figure **7** displays the SIFT key point detection.

To determine the best method for classifying each image into its respective class, the training procedure examines training data of both normal and PD -affected images. The KNN and Decision Tree classifiers discriminate between normal and Parkinson's affected images. The Decision Tree K and KNN Tree are trained to distinguish normal/ abnormal affected images. 601 feature vectors, each comprising 128 dimensions, were extracted from images for training. The training steps analyse the MRI image training data to find an optimal way to classify Parkinson's affected images into their respective two classes: normal (Category 1) and abnormal (Category 2). The extracted features are utilised to categorise the photos. For testing the 192 feature vectors, each of 128 dimensions is given as input to the Decision Tree and KNN models. The normal/abnormal Parkinson's affected MRI images are decided based on the K-Nearest Neighbour.

Tables **1** and **2** shows the classification report and confusion matrix performance of normal / Abnormal classification of Parkinson images using KNN with SIFT feature. The accuracy of the KNN with SIFT feature for the classification of PD is 60.17%.

Table 1: Confusion Matrix of KNN with SIFT feature

Categories	Normal	Abnormal
Normal	65	36
Abnormal	40	51

Tables 3 and 4 present the confusion matrix and classification report performance for the normal /

Table 2: Classification Report of KNN with SIFT Feature

Categories	Accuracy (In %)	Precision (in%)	Recall (in %)	F1- Score (in %)
Normal	64.35	64.32	61.94	63.07
Abnormal	56.04	56.00	58.62	56.28
Avg	60.19	60.16	60.28	59.67

Abnormal classification of Parkinson images using a Decision Tree with SIFT features. The Decision Tree with SIFT feature has a 64.42% classification accuracy for PD.

Table 3: Confusion Matrix of Decision Tree with SIFT Feature

Categories	Normal	Abnormal
Normal	76	25
Abnormal	42	49

Table 4: Classification Report of Decision Tree with SIFT Feature

Categories	Accuracy (In %)	Precision (In %)	Recall (In %)	F1- Score (In %)
Normal	75.00	75.21	64.43	69.38
Abnormal	53.84	53.82	66.21	59.35
Avg	64.42	64.51	65.32	64.36

This study's relatively low performance (60-64%)can be explained by the subtle and diffuse nature of PD-related structural changes in MRI images, even though SIFT has demonstrated robustness in general object detection and scene classification. Unlike natural images that contain distinct edges, corners, and scale-invariant key points, brain MRI scans exhibit smooth grayscale intensity variations and minimal local contrast, which limit SIFT's ability to identify distinctive key points.

4.3.2. Performance of LBP with KNN and Decision Tree Classifiers

Images of PD were used to extract LBP characteristics. The input to LBP is now the 256×256 converted image. The image is initially converted to grayscale using the LBP texture descriptor, which operates within a stable 3 × 3 pixel neighborhood. The centre pixel is then selected and thresholded against its eight-pixel neighborhood. The value is set to 1 if the intensity of the central pixel is greater than or equal to that of its neighbors, and to 0 otherwise.

Eight neighbors are subjected to the binary test, and the results are saved in an 8-bit array before being transformed to a decimal number. Both uniform and non-uniform transitions are carried out using LB. Over the LBP array, a 256-bin histogram is calculated. LBP is used to extract a 59-dimensional feature vector for a single image. We obtained a 601 × 59 matrix by using 601 photos for training. The KNN and Decision Tree classifiers are used to compile extracted features. One hundred ninety-two images were taken for testing. The KNN and Decision Tree classifiers classify both normal and pathological conditions of PD. The confusion matrix and performance metrics of the KNN with LBP feature are displayed in Tables 5 and 6. The accuracy of the KNN with LBP was 93.72%.

Table 5: Confusion Matrix of KNN with LBP Feature

Categories	Normal	Abnormal
Normal	95	6
Abnormal	6	85

Table 6: Classification Report of KNN with LBP Feature

Categories	Accuracy (In %)	Precision (In %)	Recall (In %)	F1- Score (In %)
Normal	94.05	94.00	98.00	94.00
Abnormal	93.40	93.41	93.41	93.4
Avg	93.72	93.70	95.70	93.7

Tables **7** and **8** show the confusion matrix and performance measures of KNN with LBP feature. The Decision Tree with LBP achieved an accuracy of 97.41%.

Table 7: Confusion Matrix of Decision Tree with LBP Feature

Categories	Normal	Abnormal
Normal	98	3
Abnormal	2	89

Table 8: Classification Report of Decision Tree with LBP Feature

Categories	Accuracy (In %)	Precision (In %)	Recall (In %)	F1- Score (In %)
Normal	97.02	97.00	98.00	97.49
Abnormal	97.80	97.81	97.80	97.39
Avg	97.41	97.40	97.90	97.44

4.4. Performance Comparison

Comparative studies on CNN and autoencoderbased systems have demonstrated similar improvements in accuracy for disease detection tasks [14–17]. Likewise, recent Al-driven CNN models have proven highly effective in automating complex medical image diagnoses such as lung cancer detection, further reinforcing the potential of deep learning in neuroimaging-based disease prediction [18].

A comparative study of two different feature extractions, namely, SIFT and LBP, on the Decision Tree and KNN. It is noted that the highest accuracy of 97.41 % is obtained with the Decision Tree using LBP features. Table **9** shows the overall performance of the LBP and SIFT features with KNN and Decision Tree. The comprehensive comparison of this work is displayed in Figure **7**.

Table 9: Overall Performance of the KNN and Decision Tree with SIFT and LBP Features

Features	Classifier	Accuracy (in %)
LBP	KNN	93.72
LDF	Decision Tree	97.41
SIFT	KNN	60.19
SIFI	Decision Tree	64.42

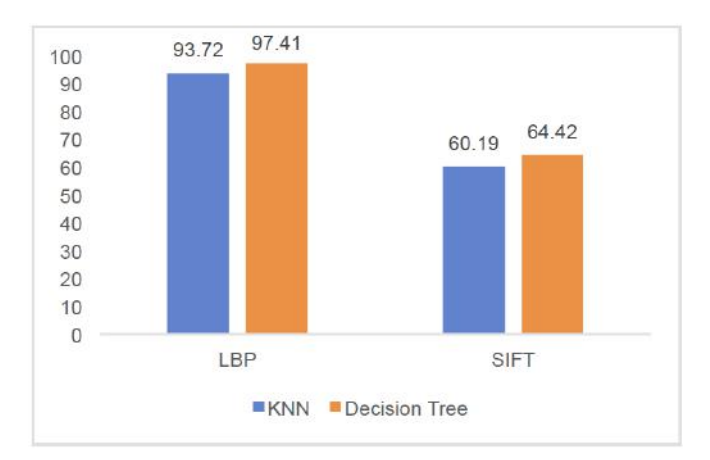
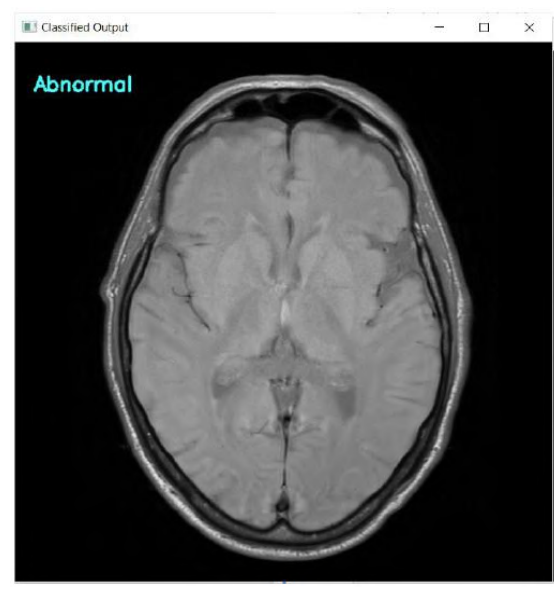


Figure 7: Overall comparison of the proposed work.

Testing Sample Output

The sample output of the prediction of PD is displayed in Figure 8.



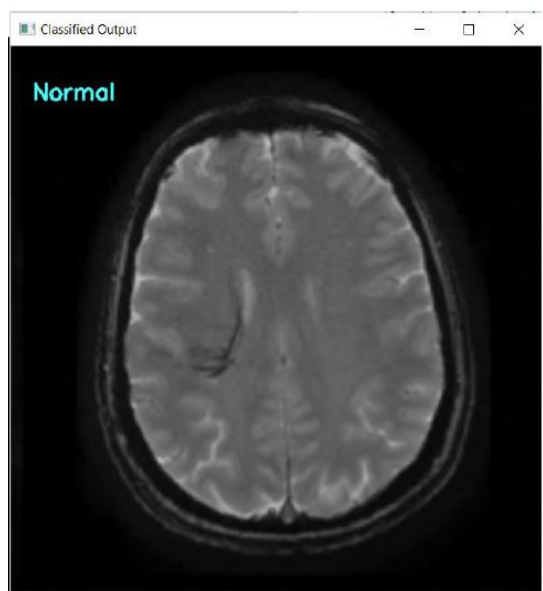


Figure 8: Sample output of the proposed work.

5. CONCLUSION

The suggested approach confirms that cutting-edge Al-driven methods significantly enhance diagnostic precision in medical imaging, closely aligning with results from earlier deep learning and image-based recognition studies [14-24]. The proposed framework successfully distinguishes MRI images of patients with Parkinson's disease from those of normal individuals by combining handcrafted features, such as SIFT and LBP, with traditional classifiers, including Decision Tree and KNN. This hybrid approach shows that traditional

feature engineering can compete with modern CNN-based diagnostic systems when optimised in a structured learning environment. These findings highlight how crucial its to combine traditional and deep learning techniques for increased dependability and earlier illness detection in neuroimaging applications

REFERENCES

- [1] Mozhdehfarahbakhsh A, Chitsazian S, Chakrabati P, Chakrabarti T, Kateb B, Nami M. An MRI-based Deep Learning Model to predict Parkinson's Disease Stages. Medline 2021. https://doi.org/10.1101/2021.02.19.21252081
- [2] Pereira CR, Pereira DR, Silva FA, Hook C. A Step Towards the Automated Diagnosis of Parkinson's Disease: Analyzing Handwriting Movements. IEEE 28 International Symposium on Computer-Based Medical Systems 2015. https://doi.org/10.1109/CBMS.2015.34
- [3] Challa KNR, Pagolu VS, Panda G. An Improved Approach for Prediction of Parkinson's Disease using Machine Learning. International Conference on Signal Processing, Communication, Power and Embedded System 2016. https://doi.org/10.1109/SCOPES.2016.7955679
- [4] Shah PM, Zeb A, Shafi U, Zaidi SFA, Shah MA. Detection of Parkinson's Disease in Brain MRI using Convolutional Neural Network. Proceedings of the 24th International Conference on Automation & Computing, Newcastle University 2018. https://doi.org/10.23919/IConAC.2018.8749023
- [5] Senturk ZK. Early Diagnosis of Parkinson's Disease using Learning Algorithms. Medical Hypotheses 2020; 138. https://doi.org/10.1016/j.mehy.2020.109603
- [6] Anitha S. Improved Classification Accuracy for Diagnosing the Early Stage of Parkinson's Disease using Alpha Stable Distribution. The Institution of Electronics and Telecommunication Engineers 2021. https://doi.org/10.1080/03772063.2021.1910580
- [7] Adel E, Elmogy M, Elbakry H. Image stitching based on feature extraction techniques: a survey. International Journal of Computer Applications 2014; 99(6): 1-8. https://doi.org/10.5120/17374-7818
- [8] Lowe DG. Distinctive image features from scale invariant key points. International Journal of Computer Vision 2004; 60(2): 91-110. https://doi.org/10.1023/B:VISI.0000029664.99615.94
- [9] Chiu LC, Chang TS, Chen JY, Chang NYC. Fast SIFT designs for real-time visual feature extraction. IEEE Transactions on Image Processing 2013; 22(8): 3158-3167. https://doi.org/10.1109/TIP.2013.2259841
- [10] Fradi H, Dugelay JL. A new multiclass SVM algorithm and its application to crowd density analysis using LBP features. International Conference on Image Processing IEEE 2013; pp. 4554-4558. https://doi.org/10.1109/ICIP.2013.6738938
- [11] Vasanawala SS, Nguyen KL, Hope MD, Bridges MD, Hope TA, Reeder SB, Bashir MR. Safety and technique of Ferumoxytol administration for MRI. Magnetic Resonance in Medicine 2016; 75(5): 2107-2111. https://doi.org/10.1002/mrm.26151

- [12] Agrawal R. K-Nearest Neighbor for Uncertain Data. International Journal of Computer Applications 2014; 105(11): 13-16.
- [13] Dar SA, et al. Improving Alzheimer's Disease Detection with Transfer Learning. Int J Stat Med Res 2025; 14: 403-415. https://doi.org/10.6000/1929-6029.2025.14.39
- [14] Dar SA, Palanivel S, Geetha MK, Balasubramanian M. Mouth Image Based Person Authentication Using DWLSTM and GRU. Inf Sci Lett 2022; 11(3): 853-862. https://doi.org/10.18576/isl/110317
- [15] Dar SA, Palanivel S. Performance Evaluation of Convolutional Neural Networks (CNNs) And VGG on Real Time Face Recognition System. Adv Sci Technol Eng Syst J 2021; 6(2): 956-964. https://doi.org/10.25046/aj0602109
- [16] Dar SA, Palanivel S. Real Time Face Authentication System Using Stacked Deep Auto Encoder for Facial Reconstruction. Int J Thin Film Sci Technol 2022; 11(1): 73-82. https://doi.org/10.18576/ijtfst/110109
- [17] Dar SA, PS. Real-Time Face Authentication Using Denoised Autoencoder (DAE) for Mobile Devices 2022; 21(6): 163-176. https://doi.org/10.4018/978-1-7998-9795-8.ch011
- [18] Ayadi W, et al. Al-Powered CNN Model for Automated Lung Cancer Diagnosis in Medical Imaging. Int J Stat Med Res 2025; 14: 616-625. https://doi.org/10.6000/1929-6029.2025.14.58
- [19] Ibrahim H, Mahmoud M, Ahmad M, Mandouh R. Different Approaches for Outlier Detection in Life Testing Scenarios. Computational Journal of Mathematical and Statistical Sciences 2024; 3(1): 203-227. https://doi.org/10.21608/cimss.2024.254148.1033
- [20] Onyekwere C, Nwankwo C, Obulezi O, Ezeilo C. The feature-value paradox: Unsupervised discovery of strategic archetypes in the smartphone market using machine learning. Journal of Artificial Intelligence in Engineering Practice 2025; 2(2): 65-72. https://doi.org/10.21608/jaiep.2025.420689.1024
- [21] Raihen MN, Hossain MI, Chellamuthu V. Predicting clinical outcomes in liver cirrhosis using machine learning and data balancing technique. Computational Journal of Mathematical and Statistical Sciences 2025; 4(2): 664-696. https://doi.org/10.21608/cjmss.2025.397747.1213
- [22] Shalaby Y, Embark A. A predictive model for climate change using advanced machine learning algorithms in Egypt. Journal of Artificial Intelligence in Engineering Practice 2025; 2(2): 1-21. https://doi.org/10.21608/jaiep.2025.415474.1020
- [23] Nnaekwe K, Ani E, Obieke V, Okechukwu C, Usman A, Othman M. Forecasting seasonal rainfall with time series, machine learning and deep learning. Innovation in Computer and Data Sciences 2025; 1(1): 51-65. https://doi.org/10.64389/icds.2025.01127
- [24] Almetwally EM, Elbatal I, Elgarhy M, Kamel AR. Implications of machine learning techniques for prediction of motor health disorders in Saudi Arabia, Alexandria Engineering Journal 2025; 127: 1193-1208. https://doi.org/10.1016/j.aej.2025.07.015

Received on 12-10-2025 Accepted on 15-11-2025 Published on 01-12-2025

https://doi.org/10.6000/1929-6029.2025.14.67

© 2025 Indhumathi et al.

This is an open-access article licensed under the terms of the Creative Commons Attribution License (http://creativecommons.org/licenses/by/4.0/), which permits unrestricted use, distribution, and reproduction in any medium, provided the work is properly cited.